Gene 927 (2024) 148717

Contents lists available at ScienceDirect

Gene

journal homepage: www.elsevier.com/locate/gene

Research paper

Genome-wide identification of Fgfr genes and function analysis of Fgfr4 in myoblasts differentiation of *Lateolabrax maculatus*

Hao Li [a], Ximeng Dong [a], Lingyu Wang [a], Haishen Wen [a], Xin Qi [a], Kaiqiang Zhang [a], Yun Li [a,b,*]

[a] Key Laboratory of Mariculture, Ministry of Education (KLMME), Ocean University of China, Qingdao 266003, China
[b] Sanya Oceanographic Institution, Ocean University of China, Sanya 572000, China

ARTICLE INFO

Edited by Carolina Bonin and Eric Alexander Lewallen

Keywords:
Spotted sea bass
Fibroblast growth factor receptors
Gene family
Myogenesis
Myoblast

ABSTRACT

Fibroblast growth factor receptors (Fgfrs) are involved in cell proliferation, differentiation, and migration via complex signaling pathways in different tissues. Our previous studies showed that fibroblast growth factor receptor 4 (*fgfr4*) was detected in the most significant quantitative trait loci (QTL) for growth traits. However, studies focusing on the function of *fgfr4* on the growth of bony fish are still limited. In this study, we identified seven *fgfr* genes in spotted sea bass (*Lateolabrax maculatus*) genome, namely *fgfr1a*, *fgfr1b*, *fgfr2*, *fgfr3*, *fgfr4*, *fgfr5a*, and *fgfr5b*. Phylogenetic analysis, syntenic analysis and gene structure analysis were conducted to further support the accuracy of our annotation and classification results. Additionally, *fgfr4* showed the highest expression levels among *fgfr*s during the proliferation and differentiation stages of spotted sea bass myoblasts. To further study the function of *fgfr4* in myogenesis, dual-fluorescence in situ hybridization (ISH) assay was conducted, and the results showed co-localization of *fgfr4* with marker gene of skeletal muscle satellite cells. By treating differentiating myoblasts cultured *in vitro* with BLU-554, the mRNA expressions of myogenin (*myog)* and the numbers of myotubes formed by myoblasts increased significantly compared to negative control group. These results indicated that Fgfr4 inhibits the differentiation of myoblasts in spotted sea bass. Our findings contributed to filling a research gap on *fgfr4* in bony fish myogenesis and the theoretical understanding of growth trait regulation of spotted sea bass.

1. Introduction

The improvement of the growth performance of farmed animals have gained massive research attention over the years (Mommsen et al., 1999; Syme and Shadwick, 2011). Generally, the growth patterns of vertebrates' skeletal muscle can be classified into two types, namely determinate growth pattern and indeterminate growth pattern (Goldspink and Bourne, 1972). Unlike most higher vertebrates, which exhibit a determinate growth pattern, the skeletal musculature of many fish species sustain persistent hyperplasia and hypertrophy throughout their life, reflecting an indeterminate growth pattern (Hiebert and Anderson, 2020; Johnston, 1999). The life-long maintenance and regeneration of skeletal muscle mainly depend on muscle satellite (stem) cells (MuSCs) (Yamakawa et al., 2020). MuSCs remain dormant under resting conditions, but when stimulated by physical damage or growth signals, a portion of them become activated and rapidly re-enter the cell cycle. and they subsequently migrate, proliferate, and differentiate into myoblasts (Braun and Gautel, 2011; Dumont et al., 2015; Sambasivan et al., 2011). When myoblasts proliferate to some extent, they will exit the cell cycle, fuse with neighboring cells under the regulation of myogenin (MYOG), and eventually form multinucleated myotubes to repair the damaged muscle (Buckingham, 2006; Knight and Kothary, 2011; Zhao et al., 2006).

Fibroblast growth factor receptors (Fgfrs), are a type of

Abbreviations: aa, amino acid; BM, basic medium; bp, base pair (s); BG, the BLU-554 treatment group; cDNA, DNA complementary to RNA; CDS, coding sequence; CG, the control group; Chrs, chromosomes; DM, differentiation medium; DIG, digoxigenin; Fgfrs, fibroblast growth factor receptors; Fgfs, fibroblast growth factors; *pax7a*, paired box 7a; *pax7b*, paired box 7b; GFF, general feature format; GM, growth medium; Ig, Immunoglobulin (s); ISH, in situ hybridization; JTT, Jones-taylor-thornton; kDa, kilodalton; MS222, ethyl 3-aminobenzoate methanesulfonic acid; MuSCs, muscle satellite (stem) cells; MW, molecular weight; myog, myogenin; NJ, Neighbor-joining; NR, non-redundant; ORF, open reading frame; PBS, hosphate-buffered saline; PFA, paraformaldehyde; pI, isoelecric point; PKc-like, Protein Kinase; qPCR, quantitative real-time PCR; TM, transmembrane; TK, tyrosine kinase; UTR, untranslated region (s.

* Corresponding author.
E-mail address: yunli0116@ouc.edu.cn (Y. Li).

https://doi.org/10.1016/j.gene.2024.148717
Received 29 February 2024; Received in revised form 29 May 2024; Accepted 19 June 2024
Available online 20 June 2024

transmembrane receptors and members of tyrosine kinase receptor family (Eswarakumar et al., 2005). By binding to theirs ligands, fibroblast growth factors (Fgfs), Fgfs-Fgfrs can regulate the process of cell proliferation, differentiation, and migration via complex signaling pathways in different tissues (Muenke and Schell, 1995). So far, 5 types of FGFRs have been discovered in animals, including FGFR1, FGFR2, FGFR3, FGFR4, FGFR5 (also known as Fibroblast growth factor receptor like 1, FGFRL1) (Trueb, 2011; Wiedemann and Trueb, 2000). In teleosts, like zebrafish, a total of 7 *fgfr*s within these 5 types were identified, which are *fgfr1a*, *fgfr1b*, *fgfr2*, *fgfr3*, *fgfr4*, *fgfr5a*, and *fgfr5b* (Hall et al., 2006; Rohner et al., 2009). In higher vertebrates, the *FGFR4* gene has been well documented as an important regulator of skeletal muscle cell proliferation and differentiation (Marics et al., 2002; Zhao et al., 2006). For instance, *Fgfr4* gene is highly expressed in mouse myoblasts and regulates skeletal muscle development by affecting the activated state of muscle satellite cells (Phelps et al., 2016; Yablonka-Reuveni et al., 2015). Although its mechanism of function in fish skeletal muscle has not been reported, our previous study found *fgfr4* showed the most significant relationship with growth trait of spotted sea bass by means of QTL fine mapping (Liu et al., 2020). Therefore, we speculated that *fgfr4* played an important part in the myogenesis of spotted sea bass.

Spotted sea bass (*Lateolabrax maculatus*), widespread alongside the coastal line of East Asia, has strong capability of disease and stress resistance (Liu et al., 2023; Wang et al., 2023). And therefore spotted sea bass has become one of the mainstay industries of mariculture in China, the national yearly production of which in 2022 was over 200,000 tones (MOA, 2023). However, the lack of inadequate studies and efforts on genetic and breeding of spotted sea bass, is undermining the development of this industry and impeding the increase in yield (Zhang et al., 2023a, 2023b). Therefore, there is an urgent need to conduct further research on the genetic improvement of spotted sea bass.

In the present study, bioinformatics tools and methods were used to identify the *fgfr* family of spotted sea bass and analyze the characteristics of their evolutionary relationship, and gene structure. Additionally, qPCR and dual-fluorescence in situ hybridization was conducted to study the function of *fgfr4* in skeletal muscle generation. The results provide a theoretical basis for revealing the molecular mechanism of *fgfr4* on the growth regulation in spotted sea bass.

2. Materials and methods

2.1. Experimental fish and Ethics statement

A total of 13 healthy spotted sea bass juveniles (12–13 cm in length and 28–30 g in weight) were used in this study, which were obtained from Shuangying Aquatic Seedling Co., Ltd. (Dongying, China). Before sampling, the experimental fish were anesthetized with 100 ng/ml ethyl 3-aminobenzoate methanesulfonic acid (MS222). Efforts were made to minimize the suffering of the experimental fish during the sampling process. All the animal specimens and experimental procedures used in this study were approved by the Animal Research and Ethics Committees of Ocean University of China (Permit Number: 20141201). There were no endangered or protected species included in the present study.

2.2. Identification and sequence analysis of spotted sea bass fgfr gene family

To identify the *fgfr* genes in spotted sea bass, the amino acid sequences of Fgfr proteins of several species were downloaded from NCBI (https://www.ncbi.nlm.nih.gov/) and Ensembl (https://www.ensembl.org/) database, which were human (*Homo sapiens*), house mouse (*Mus musculus*), zebrafish (*Danio rerio*), large yellow croaker (*Larimichthys crocea*) and Nile tilapia (*Oreochromis niloticus*). The cDNA sequences of candidate *fgfr* genes of spotted sea bass were obtained by using online TBLASTN program with e-value of $E = 1e^{-5}$ to search against genomic information of spotted sea bass (genome, accession number: PRJNA408177; RNA-Seq, accession number: SRR4409341 and SRR4409397). Then, online website ORF Finder (https://www.ncbi.nlm.nih.gov/gorf/gorf/html) were utilized to get open reading frame (ORF) prediction. To further verify the annotation result, the Smartblast program was conducted against NCBI non-redundant (NR) protein sequence database.

The online tools ExPASyPort-Param (https://web.expasy.org/protparam/) was used to analyze the protein length (amino acid), relative protein molecular weight (MW, kDa), instability index, hydropathicity, and isoelectric point (pI). TMHMM 2.0 (https://services.healthtech.dtu.dk/service.php?TMHMM-2.0) and SignalP 3.0 (https://services.healthtech.dtu.dk/service.php?SignalP-3.0) were used to predict the transmembrane domain and signal peptide of the Fgfr proteins of spotted sea bass, respectively. And the subcellular localization of spotted sea bass *fgfr* family members were predicted by online tool Cell-PLoc2.0 (https://www.csbio.sjtu.edu.cn/bioinf/Cell-PLoc-2/).

2.3. Phylogenetic, syntenic and copy number analyses

Phylogenetic analysis was performed to further confirm the annotation results and analyze the evolutionary relationships of *fgfr* genes in spotted sea bass. Full-length protein sequence of *fgfr* genes of human (*Homo sapiens*), mouse (*Mus musculus*), chicken (*Gallus gallus*), cattle (*Bos taurus)*, channel catfish (*Ictalurus punctatus*), torafugu (*Takifugu rubripes*), zebrafish (*Danio rerio*), large yellow croaker (*Larimichthys crocea*), rainbow trout (*Oncorhynchus mykiss*), Japanese medaka (*Oryzias latipes*), striped sea bass (*Morone saxatilis)* and turbot (*Scophthalmus maximus)* were downloaded from NCBI and Ensembl databases. These sequences were used to perform multiple amino acid sequence alignments through Clustal W program on MEGA 7.0 (Kumar et al., 2016) software with the default parameters. Neighbor-joining (NJ) method and Jones-taylor-thornton (JTT) model were used to construct the phylogenetic tree with percent bootstrap values derived from 1000 replications (Kumar et al., 2016). The tree was modified and beautified on the ITOL website (https://itol.embl.de/login.cgi).

Synteny analysis was conducted to provide further evidence for the gene annotations of *fgfr*s from spotted sea bass. Information on neighboring genes of *fgfr*s in zebrafish, striped sea bass and spotted sea bass was attained from their genomic database on NCBI, and was visualized by Adobe Illustration (AI) 2023. Meanwhile, the intraspecies syntenic analysis was conducted by One Step MCScanX on software TBtools (Toolbox for biologists) (Chen et al., 2023), which was also used to display the positions of the *fgfr*s on chromosomes according to the general feature format (GFF) file of the reference genome.

Copy numbers of the *fgfr* family in representative vertebrates (human, mouse, cow and chicken) and several selected teleosts (channel catfish, torafugu, zebrafish, large yellow croaker, rainbow trout, Japanese medaka, striped sea bass, turbot) were determined from Ensembl and Genomics databases and compared.

2.4. Gene structure and conserved motifs analyses

To analyze the gene structure of each member of *fgfr* genes family in spotted sea bass, structural features such as exons, introns and conserved domains were visualized through TBtools according to the information obtained from the GFF file of reference genome. Conserved domains of Fgfrs in spotted sea bass were searched using NCBI-CDD (https://www.ncbi.nlm.nih.gov/Structure/cdd/wrpsb.cgi).

Conserved motifs of *fgfr* family were searched by using MEME online tool (https://meme-suite.org/meme/tools/meme) (Bailey et al., 2015), and NCBI-CDD and TBtools were used to predict the putative function and visualize the distribution of the motifs respectively. Meanwhile, the protein secondary structure of Fgfrs was analyzed using the online software SMART (http://smart.emblheidelberg.de).

2.5. Tissue isolation and cell culture

To be specific, spotted sea bass juveniles were anesthetized with MS-222 (as mentioned in Section 2.1), and their dorsal muscle was sampled and soaked in phosphate-buffered saline (PBS) with 4 % Penicillin-Streptomycin-Gentamicin Solution (BI, Israel) immediately. Thereafter, the tissues were immersed and washed in the following solutions successively: 75 % ethanol (30 s), and PBS with 4 %, 3 %, 2 %, and 1 % Penicillin-Streptomycin-Gentamicin Solution (BI, Israel) (5 min for each). Next, the skeletal muscle tissues were cut into small pieces (1 mm^3) and placed in a 175 cm^2 standard cell culture chamber. The cells were cultured in growth medium (GM), which contained L-15 medium (G-CLONE, China), Penicillin-Streptomycin-Gentamicin Solution (BI, Israel), and 20 % fetal bovine serum (Absin, China) at 25 °C in a CO_2-free incubator (Jinghong, China). The following culture and subculture processes of cells were completed just as the protocol outlined by Zhang et al. (2022a).

2.6. Total RNA extraction and cDNA preparation

The medium was removed and the cells was washed with phosphate-buffered saline (PBS) and immediately used to extract total RNA with TRIzol reagent (Vazyme, China) according to the manufacturer's instructions. The quantity of RNA was assessed by a Biodropsis BD-1000 nucleic acid analyzer (OSTC, China) and the purity of RNA was evaluated by electrophoresis using a 1 % agarose gel. RNA was subsequently used as the template to reverse transcription to get cDNA by the use of HiScript® III SuperMix (+gDNA wiper) kit (Vazyme, China).

2.7. Quantitative real-time PCR (qPCR)

Primers of *myog* were designed using the website Primer-BLAST (https://www.ncbi.nlm.nih.gov/tools/primer-blast), and the sequences of primers are presented in Table S1. The specificity and amplification efficiency of the primers were evaluated by standard curve and melting curve analysis. The results from the melt curve analysis of the genes showed single peaks, confirming the specificity of the qPCR results. The qPCR was conducted through the use of the ChamQTM SYBR® Color qPCR Master Mix (High Rox Premixed) kit (Vazyme, China) following the manufacturer's instructions. The qPCR amplification program used was: predenaturation at 95 °C for 30 s; denaturation at 95 °C for 10 s, annealing at 60 °C for 30 s, 40 cycles. Gene *α-tubulin* was utilized as the endogenous reference gene (Wang et al., 2018). All qPCR assays were conducted in three replicates for each sample, and the relative expressions of each gene were calculated using the $2^{-\Delta\Delta Ct}$ method. The data were then analyzed using SPSS 21.0 and graphed using Graphpad prism 6.0 software respectively.

2.8. RNA-seq data analysis

The transcriptomic data of myoblasts at proliferation and differentiation stages of spotted sea bass used in this study were obtained from the NCBI SRA database (Accession number: PRJNA859992) (Zhang et al., 2022a). Filtered clean reads were aligned to the reference genome of spotted sea bass using Hisat2 (v2.1.0) with default parameters ("-q" for input file of FASTQ format, and "-S" for output file of SAM format), and the mapped reads were subsequently counted with FeatureCounts (v1.5.0) ("-p" for paired-end data; "-T 8" for 8 threads; and "-t exon" for counting the feature type of exon). The number of clean reads mapped to *fgfrs* were visualized using R (v4.3.1).

2.9. Preparation of DIG-labeled and biotin-labeled riboprobes

The *fgfr4*, *pax7a* and *pax7b* sequences were cloned and verified. Briefly, dorsal white muscle cDNA was used as the template for cloning. Primers used in this experiment were designed using the website Primer-BLAST (https://www.ncbi.nlm.nih.gov/tools/primer-blast) based on the specific region of the target gene. The PCR product was purified using FastPure Gel DNA Extraction Mini Kit (Vazyme, China), and cloned into the pCE2-TA/Blunt Zero vector (Vazyme, China). Then, the vector was transformed to *Escherichia coli* (*E. coli*) and sequenced (Sangon, China).

Subsequently, primers with recognition sequences of T7 and SP6 RNA polymerase added to their 5′ ends were then used for preparation of riboprobes. Primers information were listed in Table S1, and the primers were synthesized by Sangon Biotec (Shanghai, China). The transfected *E. coli* was utilized as template for RNA probes through PCR. Targeted DNA fragments were extracted and purified. Sense and antisense probes of *pax7a/pax7b*, and *fgfr4* mRNA were transcribed *in vitro* with digoxigenin (DIG) RNA Labeling Kit (SP6/T7) (Roche, Switzerland) and Biotin RNA Labeling Kit (SP6/T7) (Roche, Switzerland) according to the instructions of the manufacturer, respectively. The probe lengths were around 400 bp (*pax7a*: 365 bp, *pax7b*: 361 bp, and *fgfr4*: 418 bp). The specificity of the probes has been checked via ISH, with both sense and antisense probes confirmed the accuracy and specificity before the usage in the FISH (Figure S1).

2.10. Dual-fluorescence in situ hybridization (FISH) of fgfr4 and pax7a/pax7b mRNA

The skeletal muscle tissue was sampled from the back muscle below the first dorsal fin of two independent normal spotted sea bass. After rinsed by PBS, the muscle tissue was fixed in 4 % paraformaldehyde (PFA) (in PBS, pH 7.4) for 16–20 h. It was then rinsed with PBST for three times, 10 min for each. And then to dehydrated the tissue, it was immersed into 30 % sucrose until the tissue sank to the bottom of the solution. Subsequently, the dehydrated tissues were cut into 0.5 cm * 0.5 cm * 0.5 cm cube, embedded with OCT compound (SAKURA, Japan) and sectioned into 7 μm sections using frozen slicing ome (Leica, Germany).

To perform the FISH assay, the sections were deparaffinized, rehydrated and treated with a series RNase-free solutions as described by Li et al. with a few modifications (Li et al., 2024). To detect the probes labeled with DIG HRP-conjugated anti DIG Fab fragments (1:400 diluted with PBS) were employed. Afterwards, TSA staining solution containing 100 × tyramide Alexa Fluor 488 (Invitrogen, USA) was applied to the slides to show the DIG labeled mRNA with green fluorescent. After detection of the green fluorescent, the HRP was inactivated with 1 % H_2O_2 for 10 min. To detect the biotin labeled probes, the HRP-conjugated Strepatvidin (1:400 diluted with PBS) were used. TSA staining solution with 100 × tyramide Alexa Fluor 594 (Invitrogen, USA) was applied to show the red fluorescent. The sections were observed and images were taken by a fluorescence microscope (ECHO, USA).

2.11. Blocking Fgfr4 during cell differentiation

When the cells (cultured in GM) grew to approximately 80 % abundance, the culture medium was replaced with basic medium (BM) which contained L-15 and BI only. After 2 h of starvation, for the BLU-554 treatment group (BG), the BM was replaced with differentiation medium (DM) added with BLU-554 (20 nmol/ml) (Hatlen et al., 2019; Zhang et al., 2022b). Meanwhile, the control group (CG) were treated with DM only. DM contained 98 % BM and 2 % horse serum (Absin, China) (Zhao et al., 2006). Cell samples were collected when they were cultured in DM for a duration of 12 h; 24 h, 48 h and 72 h, with 3 replicate samples for each time point. The DM were changed every 24 h.

Cells were collected after being induced in DM for 72 h. After being washed with PBS, the cells were fixed with 4 % PFA, then washed by PBS for 15 min, permeabilized with 0.25 % Triton X-100 (Solelybio, China) for 20 min and washed by PBS again. Subsequently, the cells were stained with 4′, 6-diamidino-2-phenylindole (DAPI, 2 mg/mL)

(Solelybio, China) at room temperature for 2 min, followed by observed and imaging under a fluorescence microscope (ECHO, USA). Ten fields of each group were randomly selected to count the ratio of the numbers of multinucleated myotubes (with 3 nuclei per cell) to all cells in the fields.

3. Results

3.1. Identification of fgfrs in spotted sea bass

A total of 7 full-length *fgfr* genes were identified from spotted sea bass genome, which are *fgfr1a*, *fgfr1b*, *fgfr2*, *fgfr3*, *fgfr4*, *fgfr5a*, and *fgfr5b*. A summary of the characteristics of the *fgfr* members was showed in Table 1. The predicted protein lengths ranged from 494 to 945 aa, and the predicted molecular weight ranged from 54.18 to 105.90 kDa. The predicted pI varied from 5.63 to 9.31. Most of the Fgfrs were characterized as unstable and hydrophilic proteins. Signal peptide prediction showed that most of the Fgfr members contained signal peptide sequence, excluding Fgfr3. There were 2 Fgfr members (Fgfr1a and Fgfr2) containing two transmembrane structures, and the rest containing one transmembrane structure. It's worth noting that *fgfr1-4* genes shared similar CDS lengths, predicted protein lengths and subcellular localization (Lysosome and (or) Nucleus). In contrast, *fgfr5a* and *fgfr5b* are predicted to have relatively short protein sequences, and exhibit distinct differences from other *fgfr* gene members.

3.2. Phylogenetic and syntenic analyses of fgfrs in spotted sea bass

To better understand the evolutionary relationships of Fgfrs, Fgfr protein sequences of 13 species, including higher vertebrates and teleosts, were selected to conduct the phylogenetic analysis (Fig. 1). The phylogenetic tree confirmed the identification of *fgfr* genes in spotted sea bass. All the *fgfr* genes of spotted sea bass were primarily clustered with other fish and then with the higher vertebrates.

The syntenic analysis were used to further ensure the accuracy of annotations of multiple gene copies (*fgfr1a*, *fgfr1b*, *fgfr5a* and *fgfr5b*). The results showed that for these four *fgfr* genes, conserved genomic neighborhoods were found across zebrafish, striped sea bass and spotted sea bass (Fig. 2), which supported our annotations.

Additionally, the 7 *fgfr* genes of spotted sea bass were dispersed on 6 chromosomes (Chrs). Two *fgfr* genes (*fgfr3* and *fgfr5b*) were located on chr22, while the remaining *fgfr* genes were evenly distributed on chr12, 15, 16, 21 and 24 (Fig. 3).

3.3. Copy number comparison of fgfr genes in selected vertebrates

Several kinds of higher vertebrates and teleosts were selected to compare their copy numbers of *fgfr* genes. As shown in Table 2, the copy numbers of *fgfr* genes among vertebrates fluctuated between 5 and 7. Notably, 5 *FGFR* gene copies were found in all the selected higher vertebrates. However, duplicated copies of *fgfr1* and *fgfr5* appeared in almost all teleost fishes, except for the channel catfish which has a single copy of *fgfr1*.

3.4. Analysis of the gene structure and motifs of the fgfr family in spotted sea bass

We also analyzed the gene structures of *fgfr* family in spotted sea bass by visualizing the DNA sequence (CDS) and untranslated regions (UTRs). Results showed that *fgfr4* had the largest number of introns (20 introns), followed by *fgfr3* (18 introns), *fgfr2* (17 introns), *fgfr1a* (17 introns) and *fgfr1b* (16 introns), while *fgfr5a* (7 introns) and *fgfr5b* (6 introns) had fewer introns (Fig. 4A). We observed three intron splicing phases in *fgfr* genes (Fig. 4A). For *fgfr1-4* members, they contained all three kinds of intron phases, however, *fgfr5a/b* only had phase 0, and phase 2 introns. For *fgfr4*, which had the most introns, there were eight phase 0, three phase 1 and nine phase 2 introns identified along its gene sequence.

A total of 10 distinct conserved motifs of Fgfrs in spotted sea bass were gained through MEME, and their amino acid sequence and function were presented in Table S2. Motifs 1, 5, 7 and 9 were four different types of Immunoglobulin (Ig) domain, and motifs 2, 3, 4, 6, 8 and 10 belonged to the catalytic domain of Protein Kinase (PKc-like). More interestingly, as shown in Fig. 4B, the four Ig motifs, were presented in all Fgfrs of spotted sea bass, which are considered as the most conserved motifs in the whole *fgfr* family. However, PKc motifs, 2–4, 6, 8 and 10 are absent in Fgfr5a and Fgfr5b of spotted sea bass. Besides, duplicates of *fgfr1* and *fgfr5* exhibited similar intron/exon structure and intron phases, and their encoded proteins shared similar motif compositions.

Based on the prediction of conserved domains (Fig. 4C), all the spotted sea bass Fgfr proteins were composed of 3 main parts, including the extracellular domain, the transmembrane (TM) domain, and the intracellular tyrosine kinase (TK) domain, except for Fgfr5a/b. For the extracellular part, the numbers of Ig-like domains varied across Fgfrs. Fgfr2 and Fgfr4 had 2 and 4 Ig domains respectively, and the other Fgfrs had three.

In this case, the accuracy of our annotation of *fgfr* genes of spotted sea bass was supported by the results of phylogenetic, syntenic, and gene structure analyses.

3.5. Expression of fgfr family under proliferation and differentiation stages of myoblasts

Based on the RNA-seq data, all the 7 *fgfr* family members expressed in the proliferation and differentiation of myoblasts cultured *in vitro* (Fig. 5A). Compared to myoblasts cultured in GM for 72 h, a significant

Table 1
Characteristics of *fgfr* genes in spotted sea bass.

Gene name	CDS length/ bp	Predicted protein length/aa	Molecular weight/ kDa	Instability index	Aliphatic index	Hydropathicity (GRAVY)	Transmembrane domain	Signal 'peptide	Isoelectric point (pI)	Subcellular localization	Accession Number
fgfr1a	2487	828	93.03	43.89	83.08	−0.321	2	YES	6.47	Lysosome. Nucleus.	PP395750
fgfr1b	2127	708	79.08	51.72	90.86	−0.189	1	YES	6.49	Lysosome. Nucleus.	PP395751
fgfr2	2499	832	92.44	46.04	78.39	−0.397	2	YES	6.04	Lysosome. Nucleus.	PP395752
fgfr3	2538	845	94.66	47.10	83.51	−0.300	1	NO	5.72	Lysosome. Nucleus.	PP395753
fgfr4	2838	945	105.90	44.49	83.11	−0.266	1	YES	5.63	Lysosome.	PP395754
fgfr5a	1485	494	54.18	44.76	79.53	−0.380	1	YES	9.27	Cell membrane.	PP395755
fgfr5b	1530	509	56.28	39.30	79.84	−0.338	1	YES	9.31	Cell membrane.	PP395756

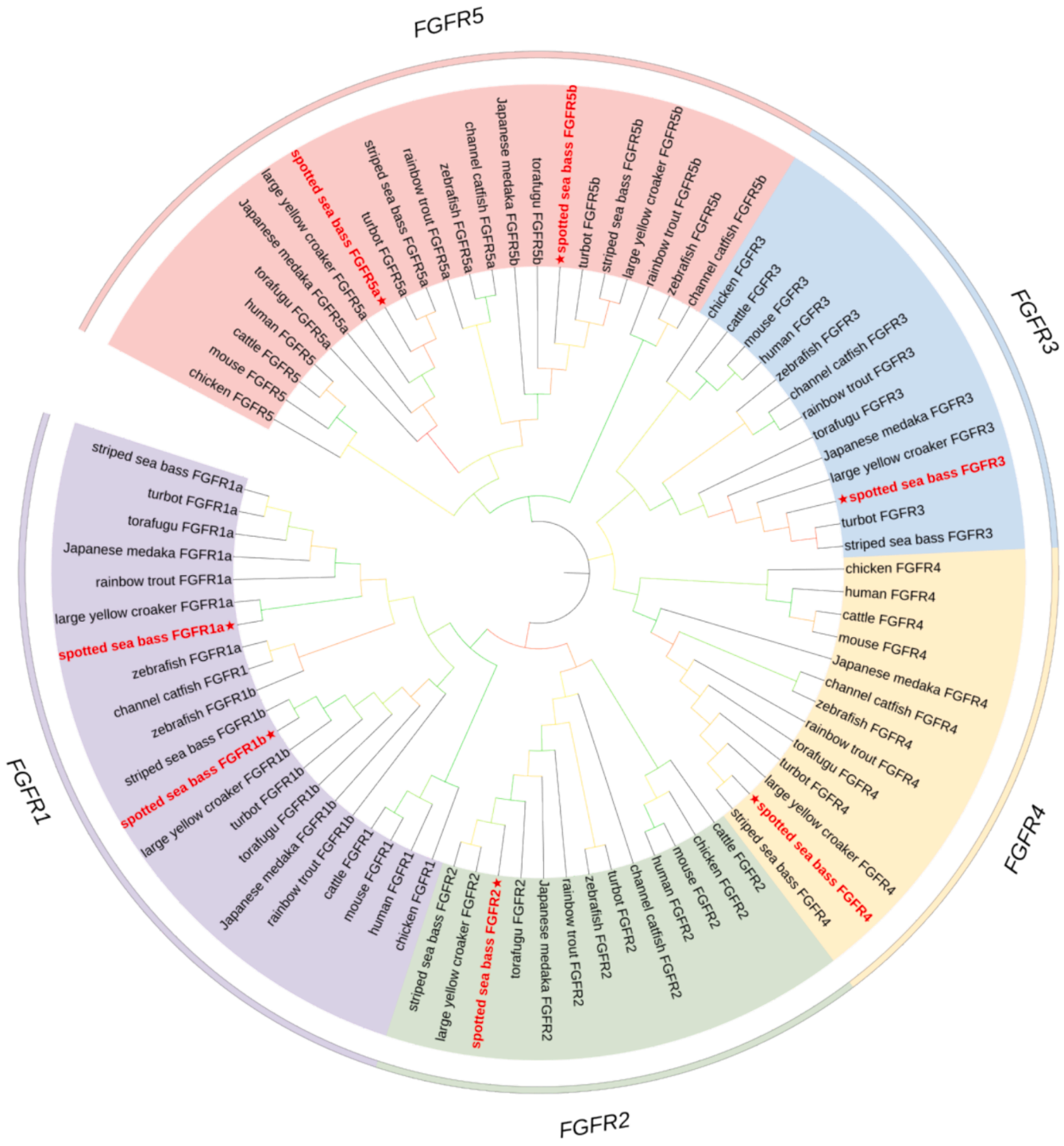

Fig. 1. Phylogenetic tree of *fgfr* family members. The *fgfr* genes of spotted sea bass are marked with bold red font and ended with a red star. Different colors of outer circle are used to mark five different clusters. Branches of different colors in the circle represent bootstrap values, and red, yellow, and green represent low, medium, and high bootstrap values, respectively.

increase in the expression of *fgfr1b* and *fgfr2* was observed, while a notable decrease in the expression of *fgfr4* and *fgfr5b* was detected in myoblasts cultured in DM for 48 h. Additionally, *fgfr4* exhibited the highest expression levels during both proliferation and differentiation stages. Therefore, the putative essential role of *fgfr4* in regulating the generation of skeletal muscle in spotted sea bass was further confirmed.

A more targeted qPCR was performed to measure the mRNA expression levels of *fgfr4* of cultured myoblasts during the transition from GM to DM (Fig. 5B). The mRNA expression of *fgfr4* exhibited a pattern of initially decreasing when cultured at GM, then increasing when switched to DM. It reached its lowest point on the first day cultured in DM and then peaked on the fourth day. This indicates that the expression of *fgfr4* decreased during the process of myoblasts proliferation, but increased during the differentiation process.

It's worth noting that *fgfr4* was expressed higher in the proliferation stage than in the differentiation stage (Fig. 5A), mainly due to the sampling time and the dynamic expression profile of *fgfr4* during myogenesis. And this was also consistent with the qPCR results (Fig. 5B).

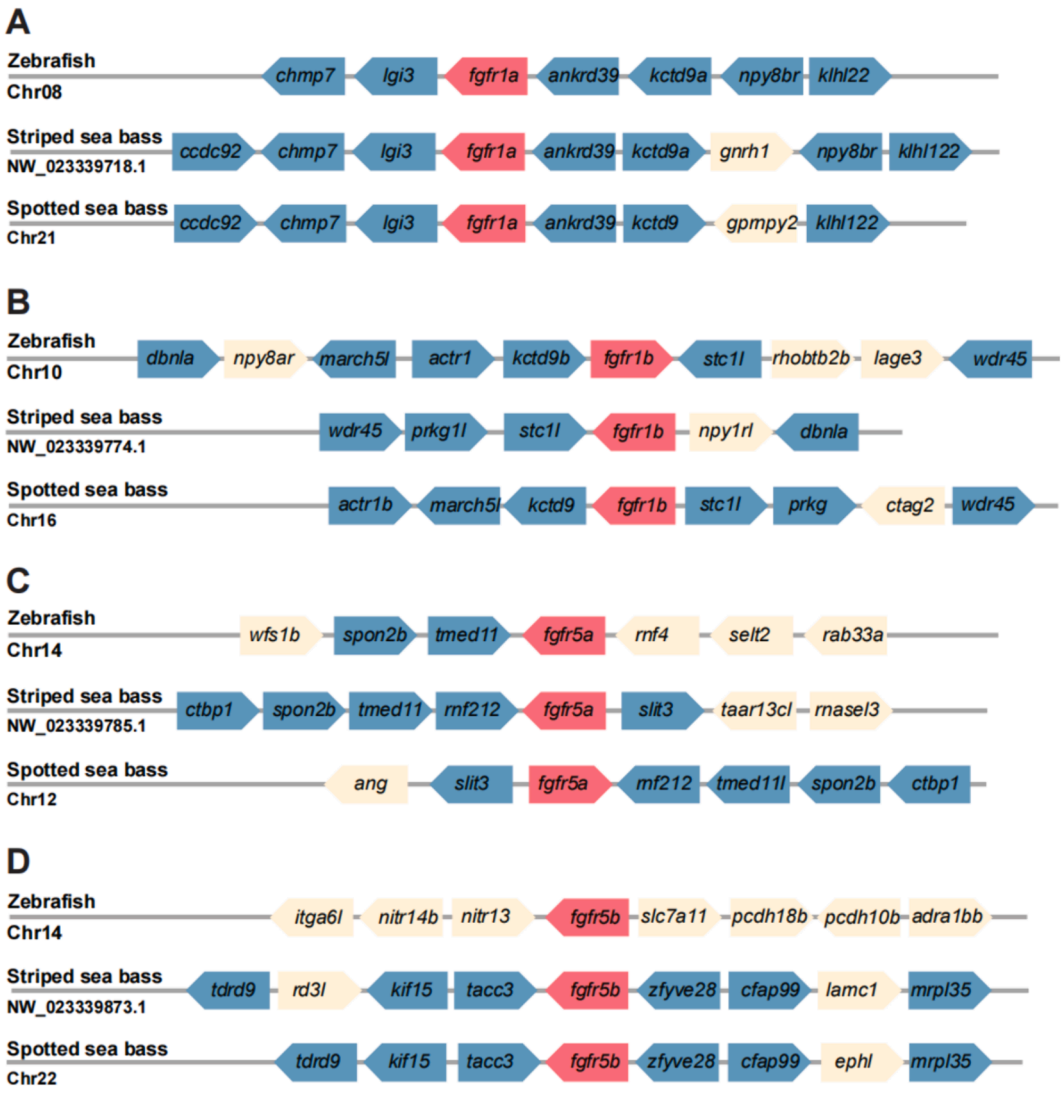

Fig. 2. Syntenic analysis of *fgfr* genes among zebrafish, striped sea bass, and spotted sea bass. A, *fgfr1a*; B, *fgfr1b*; C, *fgfr5a*; D, *fgfr5b*. The direction of the arrows indicate the gene orientation on the chromosome. The red arrows represent the *fgfr* genes, the blue arrows represent similar neighboring genes, and the light yellow arrows represent distinct neighboring genes across different genomes.

3.6. Localization of fgfr4 in muscle tissue of spotted sea bass

The cellular localization of the *fgfr4* gene in the muscle tissue of spotted sea bass was further detected. The FISH result showed that *fgfr4* co-localized with *pax7a/pax7b* (Fig. 6), which are the marker genes of skeletal muscle satellite cells, indicating that *fgfr4* gene was also expressed in skeletal muscle satellite cells. Notably, the number of cells expressing *pax7a/pax7b* gene was larger than cells expressing *fgfr4*, showing a partial co-localization result (Fig. 6).

3.7. Spotted sea bass fgfr4 inhibits differentiation of myoblasts

To investigate the role played by *fgfr4* in the differentiation of myoblasts in spotted sea bass, BLU-554, a specific antagonist for Fgfr4, was incorporated with DM to cultrure the myoblasts from the BG group, while the myoblasts in the CG group were treated with DM only. The cells of both groups were collected at 12 h, 24 h, 48 h and 72 h for the expression detection of *myog*, the marker gene of myogenic differentiation. As shown in Fig. 7A, for both the BG and CG groups, the relative expression levels of *myog* increased over time during the culture of cells in DM. Remarkably, at 12 h and 24 h, the expressions of *myog* between the BG and CG groups showed no significant difference, while the expression of myog in the BG group was significantly higher than it in the CG group at 48 and 72 h ($P < 0.05$).

At the same time, the differentiation status of myblast cells was also observed through a fluorescence microscope. In the BG group, there were more nuclei in each multinucleated myotubes and the myotubes were much longer than which in CG group. However, in CG group, myotubes were shorter and fragmented, and the majority of the myoblasts did not fuse into myotubes (Fig. 7B-C). DAPI nuclear staining showed that the number of multinucleated myotubes in BG group increased significantly ($P < 0.05$) compared with CG group. In conclusion, the expression levels of *myog* and the numbers of multinucleated myotubes both indicate that *fgfr4* inhibits the differentiation of myoblasts.

4. Discussion

4.1. Spotted sea bass fgfr family

By aligning the amino acid sequences of *fgfr* genes from several model animals, we identified 7 *fgfr* genes (*fgfr1a*, *fgfr1b*, *fgfr2*, *fgfr3*, *fgfr4*, *fgfr5a*, *fgfr5b*) in spotted sea bass genome, consistent with the results from zebrafish (Hall et al., 2006; Rohner et al., 2009). The accuracy

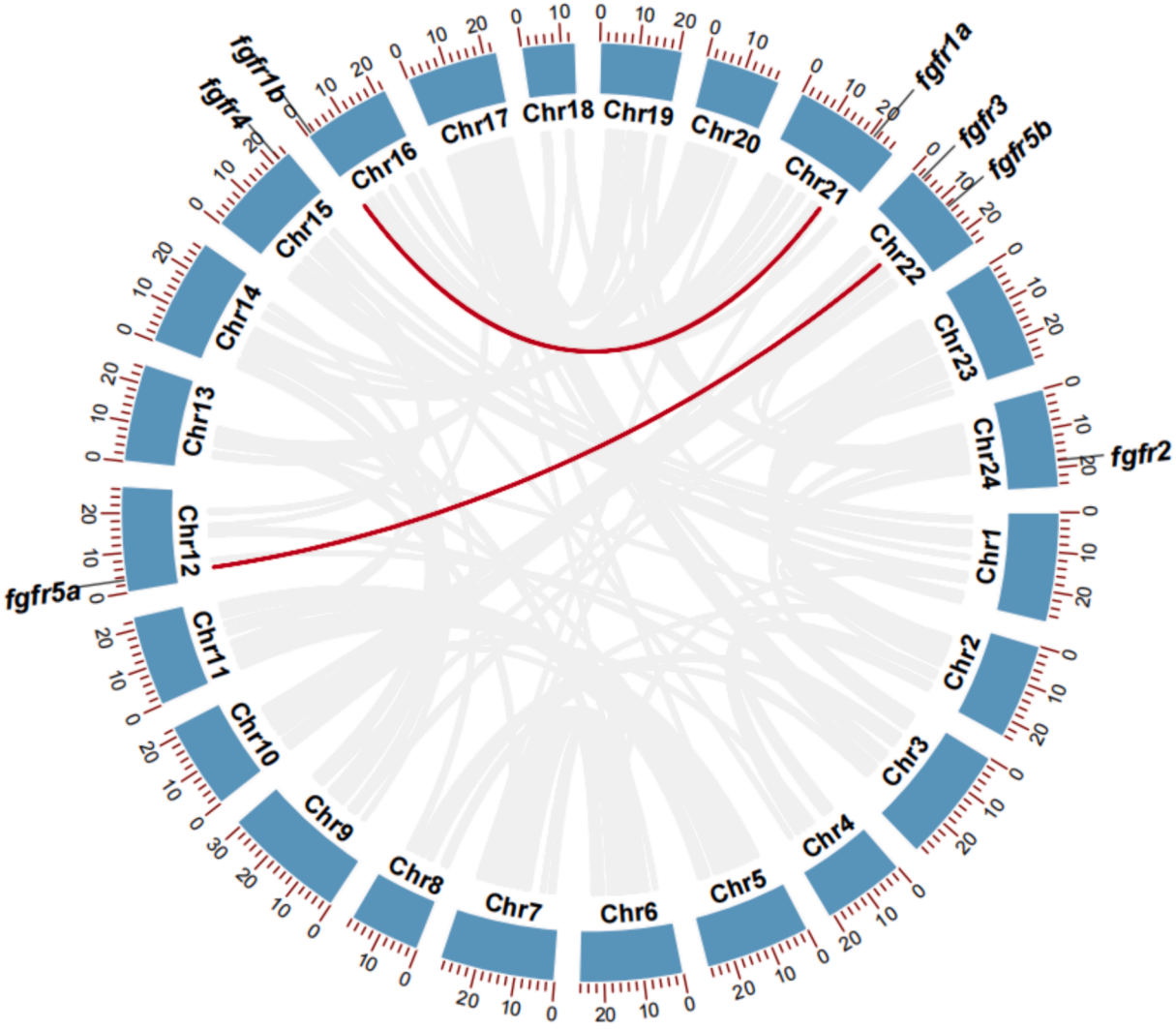

Fig. 3. Chromosomal locations and duplication modes among the *fgfr* genes of spotted sea bass. Chromosomes are represented by blue boxes. Genomic synteny is displayed in gray lines, and segmental duplication *fgfr* genes are connected with solid red lines.

Table 2
Copy numbers of *fgfr* genes in several representative vertebrates.

species	*fgfr1*	*fgfr2*	*fgfr3*	*fgfr4*	*fgfr5*	Total
Human	1	1	1	1	1	5
Mouse	1	1	1	1	1	5
Chicken	1	1	1	1	1	5
Cattle	1	1	1	1	1	5
Channel catfish	1	1	1	1	2	6
Torafugu	2	1	1	1	2	7
Zebrafish	2	1	1	1	2	7
Large yellow croaker	2	1	1	1	2	7
Rainbow trout	2	1	1	1	2	7
Japanese medaka	2	1	1	1	2	7
Striped sea bass	2	1	1	1	2	7
Turbot	2	1	1	1	2	7
Spotted sea bass	2	1	1	1	2	7

of the annotation and naming of the identified genes was further verified by phylogenetic, syntenic and gene structure analysis. The phylogenetic analysis showed that teleosts (except channel catfish) had two distinct genes copies of *fgfr1* and *fgfr5* clustering together, which is consistent with the occurrence of whole-genome duplication at the base of teleost evolution. Whole-genome duplicates have been frequently observed during metazoan evolution, and a specific duplication event occurred in fish (Meyer and Van de Peer, 2005). Whole-genome duplication is considered an efficient mechanism for increasing the genetic material available for further evolution (Trueb et al., 2005). Despite the occurrence of whole-genome duplication, not all duplicated genes were maintained, and some duplicates of the gene family were lost again during evolution (Cheng et al., 2022; Wang et al., 2020). This phenomenon may explain the single-copy status of other genes within the *fgfr* family.

4.2. The structure of Fgfrs in spotted sea bass

In humans, most Fgfr proteins consist of three parts: an extracellular domain, a single transmembrane domain, and an intracellular tyrosine kinase domain. The extracellular domain is composed of either two or three Ig-like loop domains (Mohammadi et al., 2005; Turner and Grose, 2010). The functional domain and structure analysis of Fgfrs in spotted sea bass show consistency with those in humans. Notably, according to our results, Fgfr4 of spotted sea bass has four Ig domains in its extracellular part, showing its specificity compared to other Fgfrs (Fig. 5C).

What needs to be clarified is that Fgfr5 is not a typical member of Fgfr family, showing considerable differences from the other four members in gene structure and predicted protein secondary structure. FGFR5 was firstly identified in human cartilage cDNA libraries in 2000, and was named FGFRL1 (FGFR-like 1) for its similar structure to the FGFR1

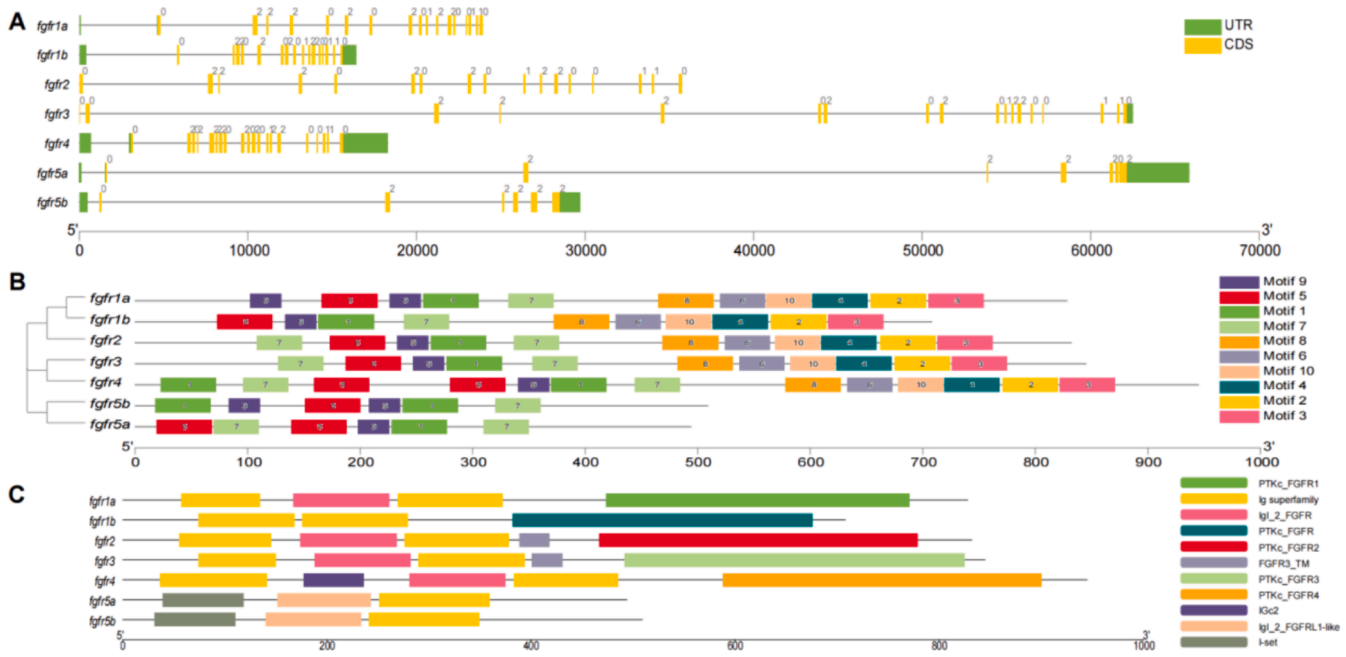

Fig. 4. Analyses of conversed motif and gene structure of Fgfr family in spotted sea bass. A, The gene structure of *fgfr*s. B, The distribution of 10 conserved motifs. C, The distribution of conversed domains. UTRs (untranslated regions) and CDSs (coding sequences) were represented as different color rectangles and black lines represented introns. PTKc, catalytic domain of the protein tyrosine kinase; Ig, immunoglobulin domain; Igl_2, second immunoglobulin (Ig)-like domain; TM, transmembrane domain; IGc2, immunoglobulin C-2 type domain; I-set, immunoglobulin I-set domain.

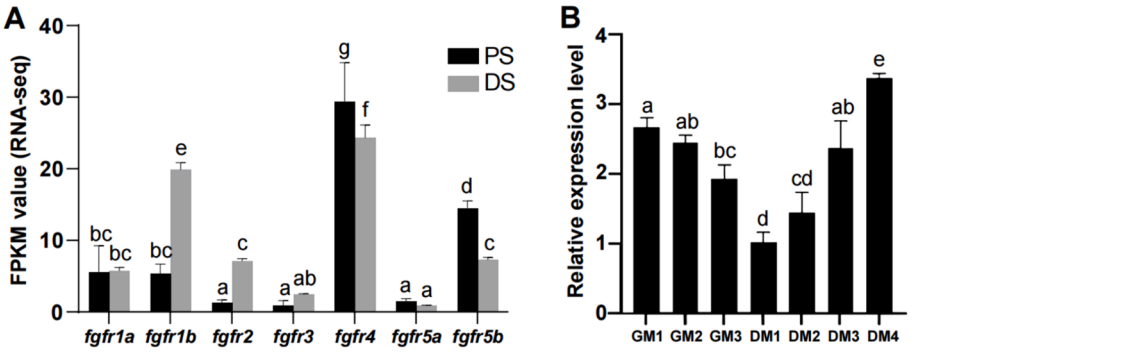

Fig. 5. The expression of *fgfr* family members of spotted sea bass during myogenesis. A, The expression of *fgfr* genes in skeletal muscle cells at the proliferation stage (PS) and differentiation stage (DS) in spotted sea bass. B, The chronological expression of *fgfr4* in proliferating and differentiating myoblasts over the time course. Myoblasts at PS were sampled after culturing the cells in growth medium for 72 h, and DS samples were collected after transferring the cells to differentiation medium for 48 h. GM1-3: Myoblasts cultured in growth medium (GM) for 24 h, 48 h and 72 h, respectively. DM1-4: Myoblasts cultured in differentiation medium (DM) for 24 h, 48 h, 72 h, and 96 h, respectively. The data are shown as the mean ± S.E.M. (n = 3), and different letters above error bars indicate significant differences ($p < 0.05$).

(Wiedemann and Trueb, 2000). One year later, other two teams found FGFRL1 from mouse, and termed it FGFR5 in order to distinguish it with FGFR1 (Kim et al., 2001; Sleeman et al., 2001). As presented in gene and protein structure analyses, Fgfr5 proteins in spotted sea bass lack the intracellular tyrosine kinase domain and have no receptor activity, which is consistent with the structure of FGFR5 in humans (Zhuang et al., 2010). Although Fgfr5 has been known for over two decades, it is still not universally recognized as a member of Fgfr family, with quite a few articles describing only four members in this family (Gabler et al., 2022; Leerberg et al., 2019; Levine et al., 2020). However, to provide more comprehensive information and highlight the distinctions among them, we considered Fgfr5 as a member of the Fgfr family in this study.

4.3. Spotted sea bass *fgfr4* expressed in satellite cells

In the present study, all seven *fgfr* genes were detected to be expressed during the proliferation and differentiation periods in skeletal muscle of spotted sea bass. The expression of *fgfr1b* was relatively higher during the differentiation stage, while *fgfr4* was expressed at the highest level in both stages. In rats, FGFR1 and FGFR4 were mainly detected to be expressed in skeletal muscle among the five types of receptors in the FGFR family (Martelly et al., 2000). The FGFR1 signaling pathway mainly plays a role in promoting proliferation and inhibiting differentiation (Cai et al., 2020; Scata et al., 1999). In adult mouse and chick, studies found that *Fgfr4* was highly expressed in muscle satellite cells to influence the proliferation and differentiation of muscle (Phelps et al., 2016; Yablonka-Reuveni et al., 2015; Zhang et al., 2018). According to our previous studies, *fgfr4* has the highest relevance with body mass and body length by constructing a high-density linkage map and performing QTL fine mapping (Liu et al., 2020). Additionally, an increase in expression of *fgfr4* was observed when the myoblasts was switched to DM (Fig. 5B), which was also detected in differentiating mouse

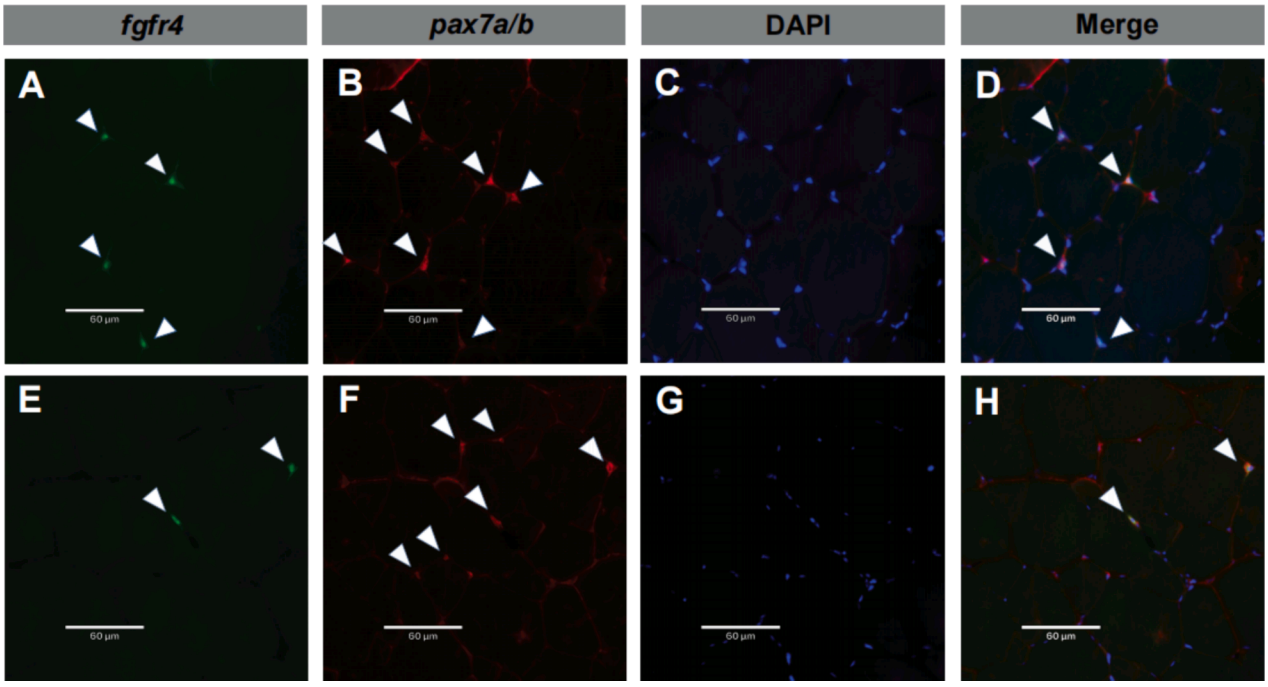

Fig. 6. Dual-fluorescence in situ hybridization of *fgfr4* and *pax7a/pax7b* in muscle tissue of spotted sea bass. A and E, Localization of *fgfr4* mRNA (green regions, stained with Alexa Fluor 488). B and F, Localization of *pax7a* mRNA (B), and *pax7b* mRNA (F) (red regions, stained with Alexa Fluor 594). C and G, Localization of cell nucleus (blue regions, stained with DAPI (4′, 6-diamidino-2-phenylindole)). D and H, Co-expression signals of *fgfr4* and *pax7a/pax7b* (indicated by the white arrowheads). Scale bars = 60 μm.

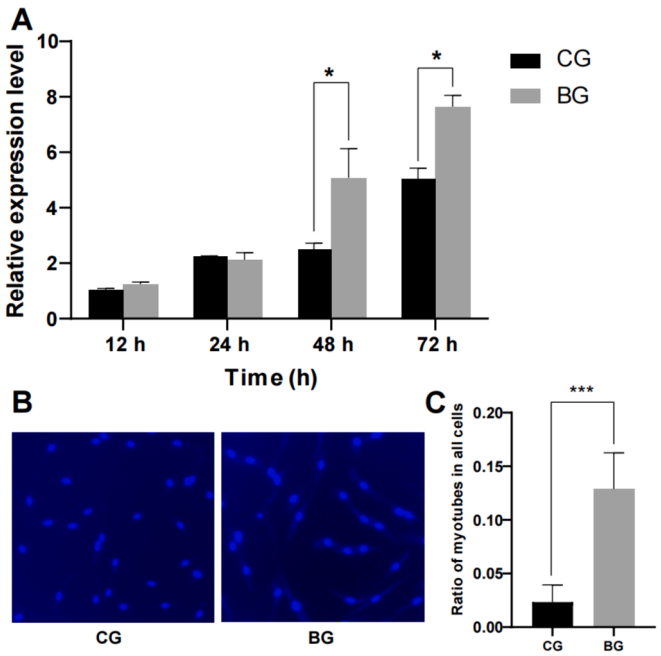

Fig. 7. Effect of Fgfr4 specific antagonist BLU-554 on differentiation of myoblasts. A, The myogenin (*myog*) expression levels of myoblasts treated with BLU-554 at 12 h, 24 h, 48 h and 72 h. B, The fluorescence assay of myoblasts at 72 h after treatment with BLU-554. C, Proportion of myotubes after induced differentiation for 72 h. CG, the control group in which the myoblasts were treated with differentiation medium (DM) only. BG, the BLU-554 treatment group in which the myoblasts were treated with DM supplemented with 20 nmol/ml BLU-554 antagonist. *, $p < 0.05$; ***, $p < 0.001$.

myoblasts (Cavanaugh and DiMario, 2017; Zhang et al., 2018). These previous results all indicated that *fgfr4* may play a crucial part in the growth of spotted sea bass.

Our FISH assay results suggested that *fgfr4* gene was co-localized in the same cells as *pax7a/pax7b*. Given that the expression of *pax7* is considered as a marker of skeletal muscle satellite cells (Olguin and Pisconti, 2012), and satellite cells play a crucial role in myogenesis, the co-localization of *fgfr4* in these cells confirms its association with myogenesis in spotted sea bass. This suggested that *fgfr4* may influence regeneration by regulating the proliferation and differentiation of skeletal myoblasts. However, it was noteworthy that in the FISH assay, more cells expressed *pax7a/b* than *fgfr4*. In mouse muscle, FGFR4 mRNA was reported undetectable normally, but high expression can be detected when muscle injury occurs (Zhao and Hoffman, 2004). This led us to consider the possibility that *fgfr4* was highly expressed only in activated satellite cells, with no expression in quiescent cells. These results all suggest that *fgfr4* have an important role in muscle growth and development.

4.4. *Fgfr4 inhibits the differentiation of myoblasts*

To further investigate the role of Fgfr4 in myoblast differentiation, *in vitro* cultured differentiating myoblasts were subjected to BLU-554. BLU-554 (also known as Fisogatinib) is an effective and selective specific small molecule inhibitor for Fgfr4 by specifically binding to the C552 residue located in the kinase domain of Fgfr4 (Hagel et al., 2015; Levine et al., 2020). At the onset of differentiation of myoblasts, the expression of *myog* is induced (Ciciliot and Schiaffino, 2010), indicating the advancement of the differentiation process. Compared with the negative control group, the relative expression level of *myog* in BLU-554 treatment group increased significantly ($P < 0.05$) (Fig. 7A). Additionally, the proportion of multinucleated myotubes to all cells in the BLU-554 treatment group was higher than that in the control group. These results suggest that inhibition of Fgfr4 led to an increase in *myog* expression and a higher proportion of multinucleated myotubes, indicating enhanced myoblast differentiation process. Interestingly, treating

differentiating myoblasts with Fgfr4 inhibitor could improve the differentiation process, while the expression of *fgfr4* of myoblasts was upregulated when cultured in DM (Fig. 5B). We speculated that the upregulated expressions of *fgfr4* were possibly a strategy myblasts used to counteract the effects of differentiation stimuli of DM, and similar patterns of regulation of myoblasts differentiation were also observed at Fgf2 (Jin et al., 2023), FoxO1 (Yuan et al., 2010), TMEM182 (Luo et al., 2021). These provide further evidence of the involvement of Fgfr4 in the regulation of myogenesis and support its potential role in influencing the differentiation process of skeletal myoblasts.

Previous studies about FGFR4 did not show entirely consistent findings in different models. For instance, in chicken and mouse, loss of Fgfr4 function resulted in defects of myogenesis (Marics et al., 2002; Yu et al., 2004), but *fgfr4* null mutant zebrafish was observed normal development with no evident muscle defects (Leerberg et al., 2019). However, whether in higher vertebrates or zebrafish, they all exhibit a determinate growth pattern of skeletal muscle development (Biga and Goetz, 2006). In this study, blocking Fgfr4 with BLU-554 promoted the differentiation of myoblasts of spotted sea bass. Additionally, treating differentiating myblasts with Fgf6a, Fgf6b and Fgf18, which were identified as potential ligands for Fgfr4, could also inhibit the differentiation process of myoblast in spotted sea bass (Yang et al., 2023). Therefore, Fgfr4 may play an important part in the maintenance of the indeterminate growth pattern of teleosts. Furthermore, the generation of skeletal muscle is a complex process involving various regulators and related signaling pathways, and one outcome may be caused by a multiple factors (Zhang et al., 2022a). For instance, FGFR4 could promote the differentiation of MuSCs, while synergistic effects of TGFb2, WNT9a, and FGFR4 weaken the differentiation of MuSCs (Zhang et al., 2018). Given these complexities, more studies focused on the Fgfs-Fgfr4 pathway and pure preparations *in vivo* experiment are needed to illuminate the mechanism of Fgfr4 regulating myogenesis of spotted sea bass.

5. Conclusion

In the present study, a total of 7 genes encoding Fgfr proteins were identified from spotted sea bass genome. Meanwhile, a series of analyses with respect to the family like systematic phylogenetic analysis, copy number analysis, gene structure analysis were conducted, which are helpful to support the annotations of spotted sea bass *fgfr*s and provide a reference for studies of Fgfr family in other teleosts. The transcriptomic data revealed that *fgfr4* was the most highly expressed gene among the *fgfr*s during the proliferation and differentiation stages of spotted sea bass myoblasts. Additionally, qPCR results demonstrated a decreasing trend in *fgfr4* expression levels during proliferation and an increasing trend during differentiation in myoblasts. The results of FISH experiments showed *fgfr4* and *pax7a/pax7b* partly co-localized in skeletal muscle satellite cells. In the myoblasts group treated with *fgfr4* antagonist, a higher mRNA expression level of the *myog* gene and more forming myotubes in treatment were observed compared to the control group cells. Collectively, our study indicates that *fgfr4* is important for skeletal muscle growth and can inhibit the differentiation of myoblasts. Our findings supplement the research on the absence of *fgfr4* in the myogenesis of bony fish and provide a theoretical basis for the regulatory mechanism of the growth traits in spotted sea bass.

Funding

This study was funded by the National Key Research and Development Program of China (2022YFD2400503), the Shandong Provincial Natural Science Foundation (ZR2021QC071) and the China Agriculture Research System (CARS-47-G06).

CRediT authorship contribution statement

Hao Li: Writing – original draft, Visualization, Investigation, Formal analysis. **Ximeng Dong:** Visualization, Investigation, Formal analysis. **Lingyu Wang:** Writing – review & editing. **Haishen Wen:** Supervision. **Xin Qi:** Investigation. **Kaiqiang Zhang:** Investigation. **Yun Li:** Writing – review & editing, Supervision, Methodology, Conceptualization.

Declaration of competing interest

The authors declare that they have no known competing financial interests or personal relationships that could have appeared to influence the work reported in this paper.

Data availability

Data will be made available on request.

Acknowledgments

We would like to thank the lab members who lent a helping hand to this study. And we are grateful for the constructive suggestions given by the reviewers.

Appendix A. Supplementary material

Supplementary data to this article can be found online at https://doi.org/10.1016/j.gene.2024.148717.

References

Bailey, T.L., Johnson, J., Grant, C.E., Noble, W.S., 2015. The MEME Suite. Nucleic Acids Res. 43 (W1), W39–W49. https://doi.org/10.1093/nar/gkv416.

Biga, P.R., Goetz, F.W., 2006. Zebrafish and giant danio as models for muscle growth: determinate vs. indeterminate growth as determined by morphometric analysis. Am. J. Physiol.-Regul. Integr. Compar. Physiol. 291 (5), R1327–R1337. https://doi.org/10.1152/ajpregu.00905.2005.

Braun, T., Gautel, M., 2011. Transcriptional mechanisms regulating skeletal muscle differentiation, growth and homeostasis. Nat. Rev. Mol. Cell Biol. 12 (6), 349–361. https://doi.org/10.1038/nrm3118.

Buckingham, M., 2006. Myogenic progenitor cells and skeletal myogenesis in vertebrates. Curr. Opin. Genet. Dev. 16 (5), 525–532. https://doi.org/10.1016/j.gde.2006.08.008.

Cai, Q.C., Wu, G.B., Zhu, M., Ge, H.A., Xue, C., Zhang, Q., Wu, P., 2020. FGF6 enhances muscle regeneration after nerve injury by relying on ERK1/2 mechanism. Life Sci. 248, 117465 https://doi.org/10.1016/j.lfs.2020.117465.

Cavanaugh, E., DiMario, J.X., 2017. Sp3 controls fibroblast growth factor receptor 4 gene activity during myogenic differentiation. Gene 617, 24–31. https://doi.org/10.1016/j.gene.2017.03.039.

Chen, C., Wu, Y., Li, J., Wang, X., Zeng, Z., Xu, J., Xia, R., 2023. TBtools-II: a "one for all, all for one"bioinformatics platform for biological big-data mining. Mol. Plant 16 (11), 1733–1742. https://doi.org/10.1016/j.molp.2023.09.010.

Cheng, C., Liu, F., Sun, X., Wang, B., Liu, J., Ni, X., Lu, P., 2022. Genome-wide identification of FAD gene family and their contributions to the temperature stresses and mutualistic and parasitic fungi colonization responses in banana. Int. J. Biol. Macromol. 204, 661–676. https://doi.org/10.1016/j.ijbiomac.2022.02.024.

Ciciliot, S., Schiaffino, S., 2010. Regeneration of mammalian skeletal muscle: basic mechanisms and clinical implications. Curr. Pharm. Des. 16 (8), 906–914. https://doi.org/10.2174/138161210790883453.

Dumont, N.A., Bentzinger, C.F., Sincennes, M.C., Rudnicki, M.A., 2015. Satellite cells and skeletal muscle regeneration. Compr. Physiol. 5 (3), 1027–1059. https://doi.org/10.1002/cphy.c140068.

Eswarakumar, V.P., Lax, I., Schlessinger, J., 2005. Cellular signaling by fibroblast growth factor receptors. Cytokine Growth Factor Rev. 16 (2), 139–149. https://doi.org/10.1016/j.cytogfr.2005.01.001.

Gabler, L., Jaunecker, C.N., Katz, S., van Schoonhoven, S., Englinger, B., Pirker, C., Berger, W., 2022. Fibroblast growth factor receptor 4 promotes glioblastoma progression: a central role of integrin-mediated cell invasiveness. Acta Neuropathol. Commun. 10 (1) https://doi.org/10.1186/s40478-022-01363-2.

Goldspink, G., 1972. Postembryonic growth and differentiation of striated skeletal muscle. In: Bourne, G. (Ed.), The Structure and Function of Muscle. Academic Press, New York, pp. 179–236.

Hagel, M., Miduturu, C., Sheets, M., Rubin, N., Weng, W., Stransky, N., Guzi, T., 2015. First selective small molecule inhibitor of FGFR4 for the treatment of hepatocellular carcinomas with an activated FGFR4 signaling pathway. Cancer Discov. 5 (4), 424–437. https://doi.org/10.1158/2159-8290.CD-14-1029.

Hall, C., Flores, M.V., Murison, G., Crosier, K., Crosier, P., 2006. An essential role for zebrafish Fgfrl1 during gill cartilage development. Mech. Dev. 123 (12), 925–940. https://doi.org/10.1016/j.mod.2006.08.006.
Hatlen, M.A., Schmidt-Kittler, O., Sherwin, C.A., Rozsahegyi, E., Rubin, N., Sheets, M.P., Hoeflich, K.P., 2019. Acquired on-target clinical resistance validates FGFR4 as a driver of hepatocellular carcinoma. Cancer Discov. 9 (12), 1686–1695. https://doi.org/10.1158/2159-8290.Cd-19-0367.
Hiebert, A., Anderson, J.E., 2020. Satellite cell division and fiber hypertrophy alternate with new fiber formation during indeterminate muscle growth in juvenile lake sturgeon (Acipenser fulvescens). Can. J. Zool. 98 (7), 449–459. https://doi.org/10.1139/cjz-2019-0243.
Jin, C., Yan, K., Wang, M., Song, W., Kong, X., Zhang, Z., 2023. Identification, characterization and functional analysis of fibroblast growth factors in black rockfish (*Sebastes schlegelii*). Int. J. Mol. Sci. 24 (4) https://doi.org/10.3390/ijms24043626.
Johnston, I.A., 1999. Muscle development and growth: potential implications for flesh quality in fish. Aquaculture 177 (1–4), 99–115. https://doi.org/10.1016/s0044-8486(99)00072-1.
Kim, I., Moon, S.O., Yu, K.H., Kim, U.H., Koh, G.Y., 2001. A novel fibroblast growth factor receptor-5 preferentially expressed in the pancreas. Biochimica et Biophysica Acta-Gene Struct. Exp. 1518 (1–2), 152–156. https://doi.org/10.1016/S0167-4781(00)00282-7.
Knight, J.D., Kothary, R., 2011. The myogenic kinome: protein kinases critical to mammalian skeletal myogenesis. Skelet. Muscle 1, 29. https://doi.org/10.1186/2044-5040-1-29.
Kumar, S., Stecher, G., Tamura, K., 2016. MEGA7: molecular evolutionary genetics analysis Version 7.0 for bigger datasets. Mol. Biol. Evol. 33 (7), 1870–1874. https://doi.org/10.1093/molbev/msw054.
Leerberg, D.M., Hopton, R.E., Draper, B.W., 2019. Fibroblast growth factor receptors function redundantly during zebrafish embryonic development. Genetics 212 (4), 1301–1319. https://doi.org/10.1534/genetics.119.302345.
Levine, K.M., Ding, K., Chen, L., Oesterreich, S., 2020. FGFR4: a promising therapeutic target for breast cancer and other solid tumors. Pharmacol. Ther. 214, 107590 https://doi.org/10.1016/j.pharmthera.2020.107590.
Li, J.S., Lyu, L., Wen, H.S., Li, Y., Wang, X.J., Yao, Y.J., Qi, X., 2024. Estrogen regulates the transcription of guppy isotocin receptors. Compar. Biochem. Physiol. B-Biochem. Mol. Biol. 269, 110895 https://doi.org/10.1016/j.cbpb.2023.110895.
Liu, C., Li, J.J., Qi, X., Wang, L.Y., Sun, D.L., Zhang, J.R., Wen, H.S., 2023. Cytochrome P450 superfamily in spotted sea bass: Genome-wide identification and expression profiles under trichlorfon and environmental stresses. Compar. Biochem. Physiol. D-Genomics Proteomics 46, 101078. https://doi.org/10.1016/j.cbd.2023.101078.
Liu, Y., Wang, H.L., Wen, H.S., Shi, Y., Zhang, M.Z., Qi, X., Li, Y., 2020. First high-density linkage map and QTL Fine mapping for growth-related traits of spotted sea bass (Lateolabrax maculatus). Mar. Biotechnol. 22 (4), 526–538. https://doi.org/10.1007/s10126-020-09973-4.
Luo, W., Lin, Z.T., Chen, J.H., Chen, G.H., Zhang, S.Y., Liu, M.Q., Zhang, X.Q., 2021. TMEM182 interacts with integrin beta 1 and regulates myoblast differentiation and muscle regeneration. J. Cachexia. Sarcopenia Muscle 12 (6), 1704–1723. https://doi.org/10.1002/jcsm.12767.
Marics, I., Padilla, F., Guillemot, J.F., Scaal, M., Marcelle, C., 2002. FGFR4 signaling is a necessary step in limb muscle differentiation. Development 129 (19), 4559–4569.
Martelly, I., Soulet, L., Bonnavaud, S., Cebrian, J., Gautron, J., Barritault, D., 2000. Differential expression of FGF receptors and of myogenic regulatory factors in primary cultures of satellite cells originating from fast (EDL) and slow (Soleus) twitch rat muscles. Cell. Mol. Biol. 46 (7), 1239–1248.
Meyer, A., Van de Peer, Y., 2005. From 2R to 3R: evidence for a fish-specific genome duplication (FSGD). Bioessays 27 (9), 937–945. https://doi.org/10.1002/bies.20293.
MOA, 2023. China Fisheries Statistical Yearbook 2023. Ministry of Agriculture, China.
Mohammadi, M., Olsen, S.K., Ibrahimi, O.A., 2005. Structural basis for fibroblast growth factor receptor activation. Cytokine Growth Factor Rev. 16 (2), 107–137. https://doi.org/10.1016/j.cytogfr.2005.01.008.
Mommsen, T.P., Vijayan, M.M., Moon, T.W., 1999. Cortisol in teleosts: dynamics, mechanisms of action, and metabolic regulation. Rev. Fish Biol. Fish. 9 (3), 211–268. https://doi.org/10.1023/A:1008924418720.
Muenke, M., Schell, U., 1995. Fibroblast-Growth-Factor Receptor Mutations in Human Skeletal Disorders. Trends Genet. 11 (8), 308–313. https://doi.org/10.1016/S0168-9525(00)89088-5.
Olguin, H.C., Pisconti, A., 2012. Marking the tempo for myogenesis: Pax7 and the regulation of muscle stem cell fate decisions. J. Cell Mol. Med. 16 (5), 1013–1025. https://doi.org/10.1111/j.1582-4934.2011.01348.x.
Phelps, M., Stuelsatz, P., Yablonka-Reuveni, Z., 2016. Expression profile and overexpression outcome indicate a role for betaKlotho in skeletal muscle fibro/adipogenesis. FEBS J. 283 (9), 1653–1668. https://doi.org/10.1111/febs.13682.
Rohner, N., Bercsenyi, M., Orban, L., Kolanczyk, M.E., Linke, D., Brand, M., Harris, M.P., 2009. Duplication of fgfr1 permits Fgf signaling to serve as a target for selection during domestication. Curr. Biol. 19 (19), 1642–1647. https://doi.org/10.1016/j.cub.2009.07.065.
Sambasivan, R., Yao, R., Kissenpfennig, A., Van Wittenberghe, L., Paldi, A., Gayraud-Morel, B., Galy, A., 2011. Pax7-expressing satellite cells are indispensable for adult skeletal muscle regeneration. Development 138 (17), 3647–3656. https://doi.org/10.1242/dev.067587.
Scata, K.A., Bernard, D.W., Fox, J., Swain, J.L., 1999. FGF receptor availability regulates skeletal myogenesis. Exp. Cell Res. 250 (1), 10–21. https://doi.org/10.1006/excr.1999.4506.
Sleeman, M., Fraser, J., McDonald, M., Yuan, S.N., White, D., Grandison, P., Murison, J. G., 2001. Identification of a new fibroblast growth factor receptor, FGFR5. Gene 271 (2), 171–182. https://doi.org/10.1016/S0378-1119(01)00518-2.
Syme, D.A., Shadwick, R.E., 2011. Red muscle function in stiff-bodied swimmers: there and almost back again. Philos. Trans. R. Soc. B-Biol. Sci. 366 (1570), 1507–1515. https://doi.org/10.1098/rstb.2010.0322.
Trueb, B., 2011. Biology of FGFRL1, the fifth fibroblast growth factor receptor. Cell. Mol. Life Sci. 68 (6), 951–964. https://doi.org/10.1007/s00018-010-0576-3.
Trueb, B., Neuhauss, S.C., Baertschi, S., Rieckmann, T., Schild, C., Taeschler, S., 2005. Fish possess multiple copies of fgfrl1, the gene for a novel FGF receptor. Biochim. Biophys. Acta 1727 (1), 65–74. https://doi.org/10.1016/j.bbaexp.2004.12.001.
Turner, N., Grose, R., 2010. Fibroblast growth factor signalling: from development to cancer. Nat. Rev. Cancer 10 (2), 116–129. https://doi.org/10.1038/nrc2780.
Wang, L.Y., Tian, Y., Wen, H.S., Yu, P., Liu, Y., Qi, X., Li, Y., 2020. Slc4 gene family in spotted sea bass (Lateolabrax maculatus): Structure, evolution, and expression profiling in response to alkalinity stress and salinity changes. Genes 11 (11), 1271. https://doi.org/10.3390/genes11111271.
Wang, H., Wen, H., Li, Y., Zhang, K., Liu, Y., 2018. Evaluation of potential reference genes for quantitative RT-PCR analysis in spotted sea bass (Lateolabrax maculatus) under normal and salinity stress conditions. PeerJ 6, e5631. https://doi.org/10.7717/peerj.5631.
Wang, L.Y., Zhang, X.Y., Wen, H.S., Qi, X., Sun, D.L., Li, X.Q., Li, Y., 2023. Integrated miRNA and mRNA analysis in gills of spotted sea bass reveals novel insights into the molecular regulatory mechanism of salinity acclimation. Aquaculture 575, 739778. https://doi.org/10.1016/j.aquaculture.2023.739778.
Wiedemann, M., Trueb, B., 2000. Characterization of a novel protein (FGFRL1) from human cartilage related to FGF receptors. Genomics 69 (2), 275–279. https://doi.org/10.1006/geno.2000.6332.
Yablonka-Reuveni, Z., Danoviz, M.E., Phelps, M., Stuelsatz, P., 2015. Myogenic-specific ablation of Fgfr1 impairs FGF2-mediated proliferation of satellite cells at the myofiber niche but does not abolish the capacity for muscle regeneration. Front. Aging Neurosci. 7, 85 https://doi.org/10.3389/fnagi.2015.00085.
Yamakawa, H., Kusumoto, D., Hashimoto, H., Yuasa, S., 2020. Stem cell aging in skeletal muscle regeneration and disease. Int. J. Mol. Sci. 21 (5), 1830 https://doi.org/10.3390/ijms21051830.
Yang, J., Dong, X., Wen, H., Li, Y., Wang, X., Yan, S., Qi, X., 2023. FGFs function in regulating myoblasts differentiation in spotted sea bass (Lateolabrax maculatus). Gen. Comp. Endocrinol. 347, 114426 https://doi.org/10.1016/j.ygcen.2023.114426.
Yu, S.J., Zheng, L., Trinh, D.K., Asa, S.L., Ezzat, S., 2004. Distinct transcriptional control and action of fibroblast growth factor receptor 4 in differentiating skeletal muscle cells. Lab. Invest. 84 (12), 1571–1580. https://doi.org/10.1038/labinvest.3700187.
Yuan, Y., Shi, X.E., Liu, Y., Yang, G., 2010. Over-expression of FoxO1 inhibits the differentiation of porcine skeletal muscle myoblast. Sheng Wu Gong Cheng Xue Bao = Chin. J. Biotechnol. 26 (12), 1668–1673.
Zhang, J., Wen, H., Qi, X., Zhang, Y., Dong, X., Zhang, K., Li, Y., 2022a. Morphological and molecular responses of Lateolabrax maculatus skeletal muscle cells to different temperatures. Int. J. Mol. Sci. 23 (17) https://doi.org/10.3390/ijms23179812.
Zhang, C., Wen, H.S., Zhang, Y.H., Zhang, K.Q., Qi, X., Li, Y., 2023a. First genome-wide association study and genomic prediction for growth traits in spotted sea bass using whole-genome resequencing. Aquaculture 566, 739194. https://doi.org/10.1016/j.aquaculture.2022.739194.
Zhang, Y.H., Wen, H.S., Liu, Y., Qi, X., Sun, D.L., Zhang, C., Li, Y., 2023b. Gill histological and transcriptomic analysis provides insights into the response of spotted sea bass to alkalinity stress. Aquaculture 563, 738945. https://doi.org/10.1016/j.aquaculture.2022.738945.
Zhang, W.Y., Xu, Y.Y., Zhang, L., Wang, S., Yin, B.X., Zhao, S.H., Li, X.Y., 2018. Synergistic effects of TGFβ2, WNT9a, and FGFR4 signals attenuate satellite cell differentiation during skeletal muscle development. Aging Cell 17 (4). https://doi.org/10.1111/acel.12788.
Zhang, X.J., Zhang, X.X., Han, R.K., Wang, Z.J., Yang, Q.H., Huang, Y.M., Yan, Y.X., 2022b. BLU-554, A selective inhibitor of FGFR4, exhibits anti-tumour activity against gastric cancer. Biochem. Biophys. Res. Commun. 595, 22–27. https://doi.org/10.1016/j.bbrc.2022.01.067.
Zhao, P., Hoffman, E.P., 2004. Embryonic myogenesis pathways in muscle regeneration. Dev. Dyn. 229 (2), 380–392. https://doi.org/10.1002/dvdy.10457.
Zhao, P., Caretti, G., Mitchell, S., McKeehan, W.L., Boskey, A.L., Pachman, L.M., Hoffman, E.P., 2006. Fgfr4 is required for effective muscle regeneration in vivo. Delineation of a MyoD-Tead2-Fgfr4 transcriptional pathway. J. Biol. Chem. 281 (1), 429–438. https://doi.org/10.1074/jbc.M507440200.
Zhuang, L., Falquet, L., Trueb, B., 2010. Genome-wide comparison of FGFRL1 with structurally related surface receptors. Exp. Ther. Med. 1 (1), 161–168. https://doi.org/10.3892/etm_00000026.